

Polarization correlations in the elastic Rayleigh scattering of photons by hydrogenlike ionsA. Surzhykov,¹ V. A. Yerokhin,² T. Jahrsetz,^{3,4} P. Amaro,³ Th. Stöhlker,^{1,4,5} and S. Fritzsche^{1,6}¹*Helmholtz-Institut Jena, D-07743 Jena, Germany*²*Center for Advanced Studies, St. Petersburg State Polytechnical University, St. Petersburg 195251, Russia*³*Physikalisches Institut, Ruprecht-Karls-Universität Heidelberg, D-69120 Heidelberg, Germany*⁴*GSI Helmholtzzentrum für Schwerionenforschung, D-64291 Darmstadt, Germany*⁵*Institut für Optik und Quantenelektronik, Friedrich-Schiller-Universität Jena, D-07743 Jena, Germany*⁶*Theoretisch-Physikalisches Institut, Friedrich-Schiller-Universität Jena, D-07743 Jena, Germany*

(Received 26 November 2013; published 31 December 2013)

The (elastic) Rayleigh scattering of hard x rays by hydrogenlike ions has been investigated within the framework of second-order perturbation theory and Dirac's relativistic equation. The focus of this study was, in particular, on two questions: (i) How is the polarization of scattered photons affected if the incident light is itself (linearly) polarized, and (ii) how do the nondipole contributions to the electron-photon interaction and the relativistic contraction of the wave functions influence such a *polarization transfer*? Detailed calculations were performed for Ne⁹⁺, Xe⁵³⁺, and U⁹¹⁺ targets and for photon energies up to ten times the 1s ionization threshold of the ions. From the comparison of these fully relativistic computations with the (nonrelativistic) dipole approximation we conclude that relativistic and higher-multipole effects often lead to a significant or even complete depolarization for heavy targets and at high photon energies.

DOI: [10.1103/PhysRevA.88.062515](https://doi.org/10.1103/PhysRevA.88.062515)

PACS number(s): 31.10.+z, 32.80.Wr, 31.30.jc

I. INTRODUCTION

The elastic scattering of photons by bound atomic (or ionic) electrons, also known as Rayleigh scattering, has been investigated since the mid-1930s [1]. Apart from the fundamental interest in this second-order quantum electrodynamical (QED) process, a good and quantitative understanding of its details is essential for quite a few applications, such as medical imaging, material research, and the spectroscopy of atoms, complex molecules, and even nano-objects (see Refs. [2–4], and references therein). Detailed knowledge of the Rayleigh scattering is also required in order to determine the contributions of two other $\gamma + A \rightarrow \gamma + A$ channels at high photon energies, namely, the nuclear Thomson and Delbrück scattering [5,6]. In particular, the latter process has attracted considerable interest since it proceeds via the production of virtual electron-positron pairs and might hence be used to study the nonlinear properties of the quantum vacuum.

For many decades, experimental and theoretical Rayleigh studies were focused not only on the total and angle-differential cross sections [7–13] but also on the on the *polarization effects* in elastic photon-atom scattering. However, most of the previous investigations have dealt with (just two) scenarios in which either (i) the polarization of the scattered photons was measured for unpolarized incident light or (ii) the angular distribution of the Rayleigh scattered photons was observed for some initially linearly polarized beam [14–17]. Owing to the recent advances in developing coherent light sources and efficient detection techniques, a new generation of experiments has currently become feasible, in which the polarization of *both* the incident and outgoing photons can be explored. For example, a measurement of the linear polarization of the Rayleigh scattered light for completely linearly polarized incoming x-rays has been performed recently at the PETRA III synchrotron at DESY [18]. Moreover, further experiments, based on novel-type solid-state detectors [19,20], are presently planned for heavy atomic or ionic targets and at hard x-ray energies.

In order to analyze the current and future experiments on the polarization transfer in Rayleigh scattering of x rays by high-*Z* targets, a detailed theoretical analysis is needed that accounts for the effects of relativity and of the nondipole contributions to the electron-photon interaction. The first steps towards such an analysis have been undertaken by Manakov *et al.* [21] and Safari *et al.* [22], who investigated how the polarization of the incident radiation influences the cross sections in polarization-resolved measurements. In the present work, we continue this research and explore the behavior of the polarization Stokes parameters, i.e., the observables that are available in present-day experiments. The theoretical background for the evaluation of these parameters is laid down in Sec. II within both the nonrelativistic dipole and rigorous relativistic frameworks. Even though all basic expressions are derived for the general case of a many-electron atom (or ion), here we restrict our study to the x-ray scattering by *hydrogenlike* ions. The numerical computation of the transition amplitudes for such one-electron systems is discussed in Sec. III. Results of calculations are presented later in Sec. IV for the Ne⁹⁺, Xe⁵³⁺, and U⁹¹⁺ ions in their ground state and for a wide range of photon energies. These results demonstrate that the Rayleigh scattering of completely linearly polarized light may lead to a significant reduction of the (degree of) polarization of outgoing photons. Such a *depolarization* is caused by the relativistic and mainly nondipole effects and becomes most pronounced for the backward x-ray scattering. A summary of these results and a brief outlook is given in Sec. V.

Hartree atomic units ($\hbar = e = m_e = 1$) are used throughout the paper unless stated otherwise.

II. THEORETICAL BACKGROUND

In this section, we shall first present the basic formulas that are needed for describing the angular and polarization properties of elastically scattered light. These formulas are

derived for the general case of (many-electron) open-shell atoms and ions and are later applied to hydrogenlike ions in their $1s$ ground state, as discussed in Secs. III and IV.

A. Evaluation of the transition matrix element

The theoretical analysis of the Rayleigh scattering of photons on atoms and matter is usually performed within

the Furry picture, in which the electron-nucleus interaction is directly included in the unperturbed Hamiltonian and where the coupling of the atoms to the radiation field is treated perturbatively. In this picture, the properties of the (scattered) outgoing photons can be traced back to the evaluation of the second-order transition amplitude [10,13,22–24]. For the light scattering by heavy ions (or atoms) and in the high-energy regime, moreover, the *relativistic* form of this amplitude has to be employed:

$$\begin{aligned} \mathcal{M}_{fi}(M_f, M_i) = & \sum_{\alpha_v, J_v, M_v} \frac{\langle \alpha_f J_f M_f | \hat{\mathcal{R}}^\dagger(\mathbf{k}_2, \boldsymbol{\epsilon}_2) | \alpha_v J_v M_v \rangle \langle \alpha_v J_v M_v | \hat{\mathcal{R}}(\mathbf{k}_1, \boldsymbol{\epsilon}_1) | \alpha_i J_i M_i \rangle}{E_i - E_v + \omega} \\ & + \frac{\langle \alpha_f J_f M_f | \hat{\mathcal{R}}(\mathbf{k}_1, \boldsymbol{\epsilon}_1) | \alpha_v J_v M_v \rangle \langle \alpha_v J_v M_v | \hat{\mathcal{R}}^\dagger(\mathbf{k}_2, \boldsymbol{\epsilon}_2) | \alpha_i J_i M_i \rangle}{E_i - E_v - \omega}, \end{aligned} \quad (1)$$

where $\mathbf{k}_{1,2}$ and $\boldsymbol{\epsilon}_{1,2}$ are the wave and polarization vectors of the incident and outgoing photons, respectively, and where $|\alpha_i J_i M_i\rangle$ and $|\alpha_f J_f M_f\rangle$ denote the (many-electron) states of the ion just before and after the scattering has occurred. In addition to the total angular momenta $J_{i,f}$ and their projections $M_{i,f}$, here $\alpha_{i,f}$ refers to all the additional quantum numbers as needed for a unique specification of these states. Since we shall restrict ourselves to the *elastic* scattering of the photons on the ground state of the atoms, we have $E_i = E_f$ and also assume $\alpha_i = \alpha_f$ and $J_i = J_f$, and that the atomic levels are nondegenerate.

The transition operator $\hat{\mathcal{R}}$ in Eq. (1) describes the interaction of the electrons with the electromagnetic field. It can be written as a sum of one-particle operators, which in the Coulomb gauge is given by

$$\hat{\mathcal{R}}(\mathbf{k}, \boldsymbol{\epsilon}) = \sum_m \mathbf{A}_m(\mathbf{k}, \boldsymbol{\epsilon}) = \sum_m \boldsymbol{\alpha}_m \cdot \boldsymbol{\epsilon} e^{i\mathbf{k} \cdot \mathbf{r}_m}, \quad (2)$$

where \mathbf{r}_m and $\boldsymbol{\alpha}_m = (\alpha_{x,m}, \alpha_{y,m}, \alpha_{z,m})$ are the coordinate and the vector of the Dirac matrices for the m th particle. One can further evaluate the second-order matrix element (1) if one expands the one-particle interaction operators $\mathbf{A}_m(\mathbf{k}, \boldsymbol{\epsilon})$ in Eq. (2) into partial waves. For the propagation of a photon in some direction $\hat{\mathbf{k}} = (\theta, \phi)$ with regard to the quantization (z) axis, such an expansion reads [25,26]

$$\mathbf{A}_m(\mathbf{k}, \boldsymbol{\epsilon}) = 4\pi \sum_{pLM} i^{L-|p|} [\boldsymbol{\epsilon} \cdot \mathbf{Y}_{LM}^{(p)*}(\hat{\mathbf{k}})] \boldsymbol{\alpha}_m \mathbf{a}_{LM,m}^p(k), \quad (3)$$

where $\mathbf{Y}_{LM}^{(p)}(\hat{\mathbf{k}})$ is a vector spherical harmonics [27] and where $\mathbf{a}_{LM}^p(k)$ denote the electric ($p = 1$) and magnetic ($p = 0$) multipole components of the electromagnetic field. The explicit form of these components has been discussed elsewhere in the literature [25,26,28].

By inserting multipole expansion (3) into Eqs. (1) and (2) and performing some angular momentum algebra, we can rewrite the transition amplitude as [21,25,29]

$$\mathcal{M}_{fi}(M_f, M_i) = \sum_{kq} \sqrt{2k+1} \langle kq J_f M_f | J_i M_i \rangle U_{kq}(\alpha_f J_f; \alpha_i J_i), \quad (4)$$

where the summation over index k runs from $|J_i - J_f|$ to $J_i + J_f$, $q = -k, -k+1, \dots, k$, and where the function U_{kq} is defined by

$$\begin{aligned} U_{kq}(\alpha_f J_f; \alpha_i J_i) = & \frac{(4\pi)^2}{\sqrt{2J_i+1}} \sum_{L_1 p_1} \sum_{L_2 p_2} i^{L_1+|p_1|-L_2-|p_2|} (-1)^{J_f+J_i} T_{kq}^{L_1 p_1; L_2 p_2}(\hat{\mathbf{k}}_1, \boldsymbol{\epsilon}_1; \hat{\mathbf{k}}_2, \boldsymbol{\epsilon}_2) \\ & \times \sum_{J_v} \left(\begin{Bmatrix} L_2 & L_1 & k \\ J_i & J_f & J_v \end{Bmatrix} S_{L_2 p_2, L_1 p_1}^{J_v}(\omega) + (-1)^{L_1+L_2+k} \begin{Bmatrix} L_2 & L_1 & k \\ J_f & J_i & J_v \end{Bmatrix} S_{L_1 p_1, L_2 p_2}^{J_v}(-\omega) \right). \end{aligned} \quad (5)$$

In this expression, moreover, S^{J_v} denotes a *reduced* second-order matrix element that is independent of both the spin state of the photon and the magnetic quantum number of the ion,

$$S_{L_1 p_1, L_2 p_2}^{J_v}(\pm\omega) = \sum_{\alpha_v} \frac{\langle \alpha_f J_f \| \sum_m \boldsymbol{\alpha}_m \hat{\mathbf{a}}_{L_1, m}^{p_1}(k) \| \alpha_v J_v \rangle \langle \alpha_v J_v \| \sum_m \boldsymbol{\alpha}_m \hat{\mathbf{a}}_{L_2, m}^{p_2}(k) \| \alpha_i J_i \rangle}{E_v - E_i \mp \omega}, \quad (6)$$

while T_{kq} designates an irreducible tensor in order to describe the polarization as well as the angular dependence of the scattering process. Most generally, such a tensor can be written as [21,25]

$$T_{kq}^{L_1 p_1; L_2 p_2}(\hat{\mathbf{k}}_1, \boldsymbol{\epsilon}_1; \hat{\mathbf{k}}_2, \boldsymbol{\epsilon}_2) = \{[\boldsymbol{\epsilon}_1 \cdot \mathbf{Y}_{L_1}^{(p_1)}(\hat{\mathbf{k}}_1)] \otimes [\boldsymbol{\epsilon}_2^* \cdot \mathbf{Y}_{L_2}^{(p_2)}(\hat{\mathbf{k}}_2)]\}_{kq} = \sum_{M_1 M_2} \langle L_1 M_1 L_2 M_2 | kq \rangle [\boldsymbol{\epsilon}_1 \cdot \mathbf{Y}_{L_1 M_1}^{(p_1)}(\hat{\mathbf{k}}_1)] [\boldsymbol{\epsilon}_2^* \cdot \mathbf{Y}_{L_2 M_2}^{(p_2)}(\hat{\mathbf{k}}_2)]. \quad (7)$$

This polarization tensor T_{kq} has been further evaluated in terms of the spherical harmonics by Manakov and coworkers [21,25] for an arbitrary polarization state of the incoming and scattered photons and, more recently, by us [29] for linearly polarized light. Here we shall not repeat this discussion and just refer the reader to these papers for all additional details.

B. Cross sections and polarization parameters

With the decomposition of the second-order transition amplitude (4) into products of radial and angular factors, we are now ready to analyze the properties of the Rayleigh scattered photons. We start from the differential cross section:

$$\begin{aligned} \frac{d\sigma(\hat{\mathbf{k}}_1, \boldsymbol{\epsilon}_1; \hat{\mathbf{k}}_2, \boldsymbol{\epsilon}_2)}{d\Omega} &= \frac{1}{2J_i + 1} \sum_{M_i M_f} |\mathcal{M}_{fi}(M_f, M_i)|^2 \\ &= \sum_{kq} |U_{kq}(\alpha_f J_f; \alpha_i J_i)|^2, \end{aligned} \quad (8)$$

and here we assume that the initial state $|\alpha_i J_i\rangle$ of the ion is unpolarized and that the magnetic sublevel population of the final state $|\alpha_f J_f\rangle$ remains unobserved in the scattering process. As seen from this expression and Eqs. (4)–(7), the differential cross section $d\sigma/d\Omega$ depends on both the propagation directions $\hat{\mathbf{k}}_{1,2}$ and the (two) polarization vectors $\boldsymbol{\epsilon}_{1,2}$ of the incident and outgoing photons. Therefore, Eq. (8) can be utilized in order to explore the angular and polarization properties of the scattered light for every possible setup and geometry of the measurements. In the present study, for instance, we shall consider a setup in which the incident light is completely linearly polarized. If the wave vectors \mathbf{k}_1 and the polarization vectors $\boldsymbol{\epsilon}_1$ of such a light are chosen along the z and the x axes, as shown in Fig. 1, $d\sigma/d\Omega$ simplifies considerably. Namely, for this choice of the coordinates, the differential cross section (8) depends, apart from the photon energy, on the polarization vector $\boldsymbol{\epsilon}_2$ and the (two) angles $\hat{\mathbf{k}}_2 = (\theta, \phi)$ of the outgoing photon:

$$\frac{d\sigma(\hat{\mathbf{k}}_1 = \hat{z}, \boldsymbol{\epsilon}_1 = \hat{x}; \hat{\mathbf{k}}_2, \boldsymbol{\epsilon}_2)}{d\Omega} = \frac{d\sigma(\theta, \phi, \boldsymbol{\epsilon}_2)}{d\Omega}. \quad (9)$$

If, in addition, the (Rayleigh) scattered photons are observed with a polarization-insensitive x-ray detector, the angular distribution of the emitted radiation is simply obtained by a summation over the polarization states:

$$\frac{d\sigma_0(\theta, \phi)}{d\Omega} = \sum_{\boldsymbol{\epsilon}_2} \frac{d\sigma(\theta, \phi, \boldsymbol{\epsilon}_2)}{d\Omega}. \quad (10)$$

Apart from the angular distribution, the cross section (9) can also be utilized to derive the linear polarization of the scattered photons. As usual in atomic and optical physics, the degree and direction of the linear polarization are characterized by the

two Stokes parameters P_1 and P_2 [30,31]. While parameter $P_1 = (I_0 - I_{90})/(I_0 + I_{90})$ is determined by the intensities of light, linearly polarized at an angle $\chi = 0^\circ$ or $\chi = 90^\circ$, parameter P_2 is given by a similar ratio but for $\chi = 45^\circ$ and $\chi = 135^\circ$, respectively. Here the angle χ is defined with respect to the scattering plane, as spanned by the directions of incident and outgoing photons (cf. Fig. 1). Since the intensity I_χ is proportional to the cross section $\sigma(\theta, \phi, \boldsymbol{\epsilon}_2 = \mathbf{n}_\chi)$ for the emission of a photon with the polarization vector along \mathbf{n}_χ , we obtain

$$P_1(\theta, \phi) = \frac{d\sigma(\theta, \phi, \mathbf{n}_{0^\circ})/d\Omega - d\sigma(\theta, \phi, \mathbf{n}_{90^\circ})/d\Omega}{d\sigma_0(\theta, \phi)/d\Omega}, \quad (11)$$

$$P_2(\theta, \phi) = \frac{d\sigma(\theta, \phi, \mathbf{n}_{45^\circ})/d\Omega - d\sigma(\theta, \phi, \mathbf{n}_{135^\circ})/d\Omega}{d\sigma_0(\theta, \phi)/d\Omega}. \quad (12)$$

As seen from these expressions, the Stokes parameters still depend on the direction of scattered light. In Sec. IV, therefore, we will make use of Eqs. (11) and (12) to investigate the polarization correlations in the Rayleigh scattering for different geometries. However, before we present the results from our relativistic computations below, let us briefly recall the form of parameters P_1 and P_2 and the angular distribution σ_0 as obtained within the nonrelativistic electric dipole approximation.

C. Nonrelativistic formulas

Although the nonrelativistic expressions for the cross section and polarization parameters of the Rayleigh scattered light have been discussed in the literature (see, e.g., Refs. [2,16,21–23]), let us briefly demonstrate how they follow

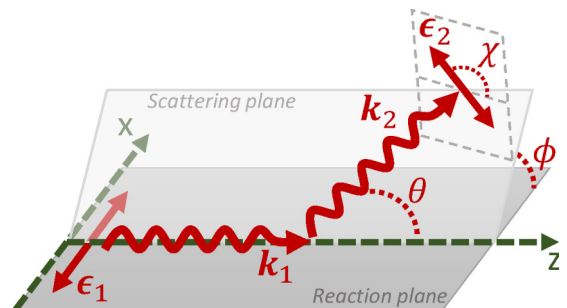


FIG. 1. (Color online) Geometry of the Rayleigh scattering for initially linearly polarized light. The wave and polarization vectors of the incoming photons define the xz plane (reaction plane), while the emission direction of the outgoing photons is characterized by the two angles, (θ, ϕ) . The direction of linear polarization of scattered light is defined with respect to the scattering plane, as spanned by vectors \mathbf{k}_1 and \mathbf{k}_2 .

rather easily from the general formulas (4)–(12). We here focus on the scattering of photons by the K -shell electrons of low- Z hydrogenlike ions for which the electron spin can be neglected in the first instance. With these two assumptions in mind, the $1s \rightarrow 1s$ transition of the ions due to the elastic scattering is described by a function U_{00} that enters the transition amplitude (4). Within leading order, i.e., if the absorbed and emitted photons are both of electric dipole type ($E1$), the angular and polarization dependence of U_{00} and hence the amplitude \mathcal{M}_{fi} arises solely from the *single* zero-rank irreducible tensor [21,29]:

$$T_{00}^{L_1=1, p_1=1; L_2=1, p_2=1}(\theta) = -\frac{\sqrt{3}}{8\pi}(\boldsymbol{\epsilon}_1 \cdot \boldsymbol{\epsilon}_2). \quad (13)$$

By inserting this expression into Eqs. (4), (5), and (8), we immediately obtain the well-known nonrelativistic formula for the cross section:

$$\frac{d\sigma^{\text{nr}}(\hat{\mathbf{k}}_1, \boldsymbol{\epsilon}_1; \hat{\mathbf{k}}_2, \boldsymbol{\epsilon}_2)}{d\Omega} \propto |(\boldsymbol{\epsilon}_1 \cdot \boldsymbol{\epsilon}_2)|^2, \quad (14)$$

which implies the angular distribution (10) of scattered photons whose polarization state remains unobserved:

$$\frac{d\sigma_0^{\text{nr}}(\theta, \phi)}{d\Omega} \propto \sin^2 \phi + \cos^2 \theta \cos^2 \phi. \quad (15)$$

Moreover, one can also use Eq. (14) to derive the Stokes parameters of Rayleigh photons:

$$P_1^{\text{nr}}(\theta, \phi) = \frac{-\sin^2 \phi + \cos^2 \phi \cos^2 \theta}{\sin^2 \phi + \cos^2 \phi \cos^2 \theta}, \quad (16)$$

$$P_2^{\text{nr}}(\theta, \phi) = \frac{2 \sin \phi \cos \phi \cos \theta}{\sin^2 \phi + \cos^2 \phi \cos^2 \theta}. \quad (17)$$

As seen from these expressions, parameter P_2^{nr} vanishes identically if the photons are emitted either within or perpendicular to the xz plane, defined by the wave and polarization vectors of the incident light. In contrast, the first Stokes parameter takes the values $P_1^{\text{nr}} = 1$ and $P_1^{\text{nr}} = -1$ for $\phi = 0^\circ$ and $\phi = 90^\circ$, which implies that the polarization of the incident light is transferred completely to the scattered photons. The validity of this nonrelativistic result will be discussed in Sec. IV, where we present our fully relativistic computations of the P_1 and P_2 polarization parameters.

III. COMPUTATIONS

As follows from our discussion above, any numerical analysis of the scattering cross sections and polarization parameters requires a computation of the reduced second-order transition amplitude (6), which involves the summation over the *complete* basis of the intermediate states $|\alpha_\nu J_\nu\rangle$. Accurate calculations of these amplitudes are rather demanding, in particular for many-electron atoms and/or large intermediate energies $E_i \pm \omega$. In the present study, we restrict ourselves to the case of relativistic hydrogenlike ions, for which the summation over the intermediate states can be performed consistently up to a high accuracy. Two independent numerical methods were employed that provided almost identical results, thus confirming the high numerical accuracy of our calculations.

The first method uses a finite-basis-set representation of the spectrum of the Dirac equation, with basis functions constructed in terms of B splines [32–35]. In this approach, the Dirac equation is solved in a spherical cavity with impenetrable walls and a radius R , which is chosen to be so large that it does not affect the calculational results. The B -spline method yields very precise results when the absolute value of the intermediate energy $|E_i \pm \omega|$ is smaller than the electron rest mass. For higher energies, however, the convergence of the results (with respect to the number of the basis functions) drops down. The reason is that the dominant contribution in this energy range comes from the Dirac continuum, which is difficult to accurately describe in any finite-basis-set method.

In the second method, the spectrum of the Dirac equation is represented by means of the Dirac-Coulomb Green's function. Here we employed the analytical representation of such a function in terms of the regular and irregular Whittaker functions [36–38]. This representation has been used in calculations by some of us, with the implementation details described in Ref. [39]. The Green's-function method is numerically more complicated than the B -spline approach, but it provides accurate results for both low and high intermediate energies.

All methods for treating the Dirac-Coulomb spectrum involve the expansion of the spectrum in partial waves (more specifically, in the angular momentum J_ν and parity P_ν of the intermediate states). It is important that contrary to the nonrelativistic case, the relativistic second-order transition amplitude contains contributions from all partial waves. For small intermediate energies $|E_i \pm \omega| \ll mc^2$, the partial-wave expansion converges very quickly, with the dominant contribution coming from just the first two to three expansion terms. In the high-energy region, however, the convergence of the expansion becomes rather slow. In the most difficult case considered here, which is Rayleigh scattering of ≈ 1.3 MeV photons by the hydrogenlike uranium, we had to take into account 20 partial waves in order to get the convergence under control.

IV. RESULTS AND DISCUSSIONS

A. Angular distributions and asymmetry ratio

Before we consider the Stokes parameters (11) and (12) for the Rayleigh scattered light, let us start with the *angular distribution* of these photons and study how it is affected by the polarization of the incident radiation. In Fig. 2, for example, we display the differential cross section (10) for the Rayleigh scattering of x-rays by hydrogenlike Ne^{9+} (top row), Xe^{53+} (middle row), and U^{91+} (bottom row) ions. Calculations have been performed for the photon energies $\hbar\omega = 1.1 I_{\text{th}}$ (solid line), $5 I_{\text{th}}$ (dashed line), and $10 I_{\text{th}}$ (dotted line), with $I_{\text{th}} \equiv I_{\text{th}}(Z)$ being the one-photon ionization threshold, and for three different geometries of the scattering process. The left column, for example, shows the angular distribution of the scattered photons if they are emitted within the xz reaction plane, as spanned by the wave and polarization vectors of the incoming radiation. For this coplanar geometry, a $\propto \cos^2 \theta$ angular distribution is predicted by the nonrelativistic dipole approach (15). However, as seen from our calculations, such an (electric dipole) emission pattern holds only for relatively light elements and photon energies not too far from the threshold energy. At increased

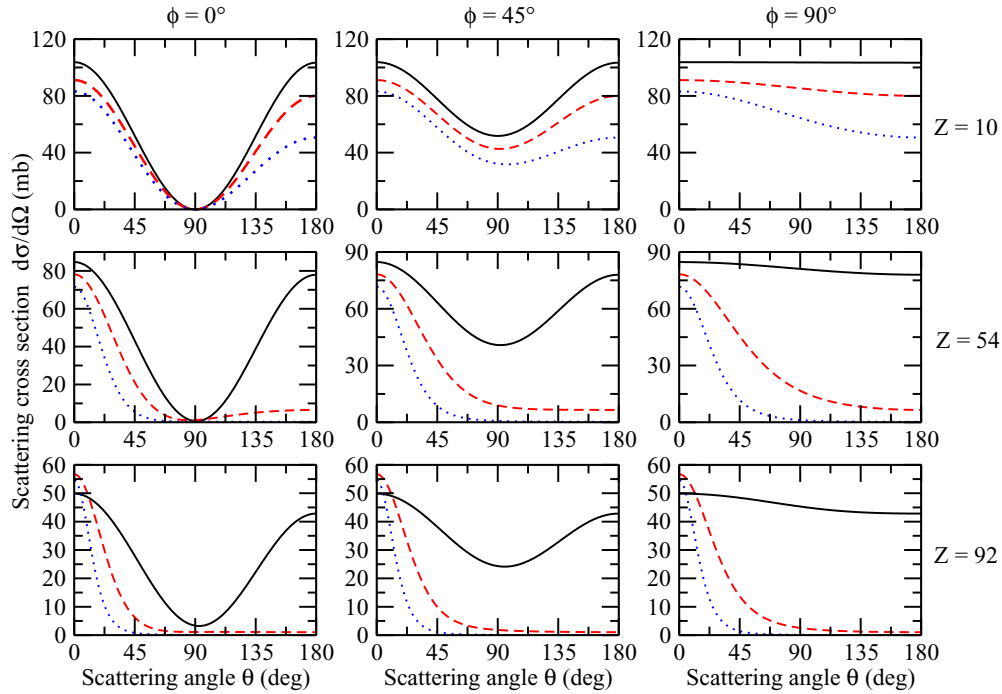


FIG. 2. (Color online) Angle-differential cross section of Rayleigh scattered linearly polarized x rays for hydrogenlike Ne^{9+} (top row), Xe^{53+} (middle row), and U^{91+} ions (bottom panel) in their ground state. Relativistic calculations were performed for three energies of the incident light, $\hbar\omega = 1.1 I_{\text{th}}$ (solid line), $5 I_{\text{th}}$ (dashed line), and $10 I_{\text{th}}$ (dotted line), where $I_{\text{th}} \equiv I_{\text{th}}(Z)$ refers to the $1s$ ionization threshold. Results are shown for different emission angles ϕ of the scattered photons with regard to the xz reaction plane: $\phi = 0^\circ$ (left column), 45° (central column), and 90° (right column); see Fig. 1.

photon energies, $d\sigma_0(\theta, \phi = 0^\circ)/d\Omega$ is no longer symmetric with regard to $\theta = 90^\circ$ but is enhanced in the forward direction. Moreover, the backscattering is significantly suppressed, and this effect is most clearly seen for the heavy ions. This *asymmetric* shift in the angular distribution of scattered photons, which was discussed before in a number of studies (see, for example, Refs. [8,12,13]), is caused mainly by the higher nondipole contributions to the electron-photon interaction operator (2). This is easily seen from the fact that the (nonrelativistic) behavior (15) is fairly well reproduced by our relativistic calculations if the multipole decomposition (3) of $\mathcal{R}(\mathbf{k}, \boldsymbol{\epsilon})$ is restricted to the electric-dipole term only ($p = 1, L = 1$).

Strong nondipole effects in the angular distribution of the elastically scattered light can be observed also for a noncoplanar “experimental” geometry. For example, in the scattering plane, perpendicular to the xz one ($\phi = 90^\circ$), these effects may *again* lead to the pronounced forward emission. Similar to what was described before, the Rayleigh emission anisotropy becomes most pronounced for the high energies, while for $\hbar\omega \approx I_{\text{th}}$ and $Z \lesssim 54$ the angular distribution $d\sigma_0(\theta, \phi = 90^\circ)/d\Omega$ is almost isotropic, as predicted by the nonrelativistic dipole approximation (15).

A series of experiments has been performed in the past to measure the angular distribution of scattered photons *within* and *perpendicular to* the xz plane (see Refs. [2,14,16], and references therein). The experimental data were usually presented in terms of the asymmetry ratio:

$$R = \frac{d\sigma_0(\theta, \phi = 0^\circ)}{d\Omega} \bigg/ \frac{d\sigma_0(\theta, \phi = 90^\circ)}{d\Omega}. \quad (18)$$

Within the nonrelativistic dipole approximation (15) and for completely polarized incident light, this ratio reads $R^{\text{nr}} = \cos^2 \theta$, independent of the nuclear charge Z and photon energy. As seen from Fig. 3, such a simple prediction holds only for relatively light elements. With the growth of the nuclear charge Z , the (absolute value of) asymmetry ratio generally decreases, and its minimum is shifted towards the forward emission angles. Again, such a departure from R_{dip} arises, to a great extent, from the higher-multipole terms in the expansion of the electron-photon interaction.

B. Polarization correlations

In addition to the angular distribution, the *linear* polarization of elastically scattered x rays can be observed in current experiments. As we mentioned already in Sec. II B, such a polarization is characterized by the Stokes parameters P_1 and P_2 . These parameters, evaluated for three photon energies in the range $1.1 I_{\text{th}} \leq \hbar\omega \leq 10 I_{\text{th}}$ and for the Xe^{53+} and U^{91+} targets, are presented in Figs. 4 and 5. As done above, calculations have been performed for the completely polarized (along the x axis) incident light and for different scattering planes, tilted by an angle ϕ with respect to the xz one. In the first column of the figures, for example, one sees the Stokes parameters of the light scattered within the plane of the incident polarization, i.e., at $\phi = 0^\circ$. In this coplanar case, the *nonrelativistic* formulas (16) and (17) predict $P_1^{\text{nr}} = 1$ and $P_2^{\text{nr}} = 0$ for all angles except $\theta = 90^\circ$, for which $d\sigma_0^{\text{nr}}(\theta = 90^\circ, \phi = 0^\circ)/d\Omega = 0$, and hence, the photon emission is forbidden. Following general symmetry properties

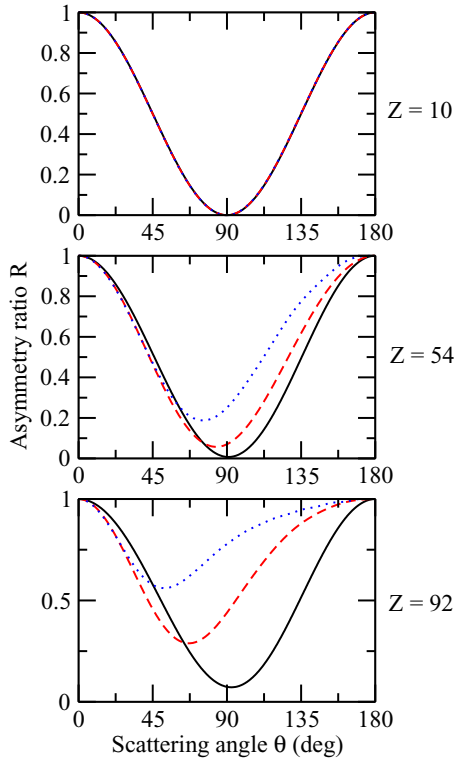


FIG. 3. (Color online) Asymmetry ratio (18) for the Rayleigh scattering of linearly polarized x rays by hydrogenlike Ne^{9+} (top), Xe^{53+} (middle), and U^{91+} ions (bottom) in their ground state. Relativistic calculations were performed for three energies of the incident light, $\hbar\omega = 1.1 I_{\text{th}}$ (solid line), $5 I_{\text{th}}$ (dashed line), and $10 I_{\text{th}}$ (dotted line); see Fig. 2.

of the scattering amplitude \mathcal{M}_{fi} (see Refs. [16,21] for details), the second parameter $P_2(\theta, \phi = 0^\circ)$ remains identically zero also within the rigorous relativistic approach. In contrast, P_1 is strongly affected by relativistic and, mainly, nondipole effects. As seen from the right column of Figs. 4 and 5, such effects lead to the decrease of the polarization, which becomes most pronounced for high photon energies, $\hbar\omega \gtrsim 5 I_{\text{th}}$, and large angles, $\theta \gtrsim 90^\circ$. In this domain and for the uranium U^{91+} target, P_1 may even become negative, thus implying that the outgoing photons are polarized perpendicular to the scattering plane. A similar tilt of the polarization, also known as the “crossover,” is also known for other radiative atomic processes such as the photoionization and radiative recombination [40–42]. Observation of such a crossover behavior for the Rayleigh scattering may be hampered, however, by a small cross section for a light emission in the backward hemisphere (see Fig. 2). For the forward angles in the range $30^\circ \lesssim \theta \lesssim 50^\circ$, where the photon yield is high, the first Stokes parameter may be reduced from $P_1^{\text{nr}} = 1$ to 0.95 for Xe^{53+} and to almost 0.8 for U^{91+} ions if the nondipole effects are taken into account. Such a depolarization is large enough to be observed with the help of available solid-state detectors.

Until now, we have explored the Stokes parameters of x rays scattered *within* the plane of polarization of incident light (xz plane). However, as was discussed in Sec. III C, a remarkable ϕ dependence of these parameters is expected in

the nonrelativistic dipole theory. For example, if the x-rays are emitted within the plane tilted by the angle $\phi = 45^\circ$, both P_1^{nr} and P_2^{nr} show strong variations as functions of the polar angle θ . Namely, while for the forward ($\theta = 0^\circ$) photon emission $P_1^{\text{nr}} = 0$ and $P_2^{\text{nr}} = 1$, they change to $P_1^{\text{nr}} = -1$ and $P_2^{\text{nr}} = 0$ for $\theta = 90^\circ$ and, further, to $P_1^{\text{nr}} = 0$ and $P_2^{\text{nr}} = -1$ for the backward angle [see Eqs. (16) and (17)]. Our relativistic calculations confirm fairly well such a behavior for the scattering of (relatively) low-energy photons by light- and medium- Z ions, as seen, for example, from the middle column of Fig. 4. However, with the growth of the nuclear charge Z and the photon energy, the higher-multipole contributions become increasingly important and lead generally to a depolarization of emitted radiation. Again, the nondipole effects are most pronounced for the large angles, $\theta \gtrsim 90^\circ$, where the variation of the Stokes parameters may reach 70%–100%. The strong depolarization can also be observed in the scattering plane, orthogonal to the xz one (cf. right columns of Figs. 4 and 5). For this geometry, the nonrelativistic predictions read $P_1^{\text{nr}}(\theta, \phi = 90^\circ) = -1$ and $P_2^{\text{nr}}(\theta, \phi = 90^\circ) = 0$ at all emission angles. While keeping P_2 unchanged, the relativistic and nondipole effects reduce the (absolute value) of P_1 , the effect which is most pronounced for energies $\hbar\omega \gtrsim 5 I_{\text{th}}$ and $\theta = 180^\circ$.

Our analysis of the Rayleigh scattering by hydrogenlike ions has been restricted so far to the case of *completely* (linearly) polarized incident light. This can be expected, for example, for the synchrotron x-rays emitted within the plane of the storage ring. In practice, however, the degree of linear polarization of synchrotron radiation is about $\mathcal{P} = 97\%–99\%$. Based on the formulas derived in Sec. II, one can investigate how the angular and polarization properties of elastically scattered photons are influenced by the variation of \mathcal{P} . Such a study is traced back to the superposition of the cross sections (8):

$$\frac{d\sigma(\theta, \phi, \epsilon_2; \mathcal{P})}{d\Omega} = \frac{1 + \mathcal{P}}{2} \frac{d\sigma(\hat{\mathbf{k}}_1 = \hat{\mathbf{z}}, \epsilon_1 = \hat{\mathbf{x}}; \hat{\mathbf{k}}_2, \epsilon_2)}{d\Omega} + \frac{1 - \mathcal{P}}{2} \frac{d\sigma(\hat{\mathbf{k}}_1 = \hat{\mathbf{z}}, \epsilon_1 = \hat{\mathbf{y}}; \hat{\mathbf{k}}_2, \epsilon_2)}{d\Omega}, \quad (19)$$

where we assume, for simplicity, that the (degree of) circular polarization of incoming x rays is identically zero. By inserting this expression into Eqs. (10), (11), and (12) one immediately derives the differential cross section and Stokes parameters that, in addition to the emission angles (θ, ϕ), also depend on the degree \mathcal{P} . Calculations made for various values of \mathcal{P} and for Rayleigh scattering of 206.7 keV ($\hbar\omega = 5 I_{\text{th}}$) photons by the hydrogenlike xenon ion are presented in Fig. 6. Here we restrict our analysis to the coplanar emission geometry, $\phi = 0^\circ$, where the single Stokes parameter $P_1(\theta; \mathcal{P})$ is nonzero. As seen from the right panel of Fig. 6, P_1 appears to be very sensitive to the degree of polarization of incident radiation. For example, an about 13%–20% reduction of the polarization of emitted photons can be observed for the forward emission angles $\theta \lesssim 45^\circ$ if \mathcal{P} just changes from 1 to 0.90. These results stress the importance of the control of polarization properties of radiation employed in elastic scattering experiments.

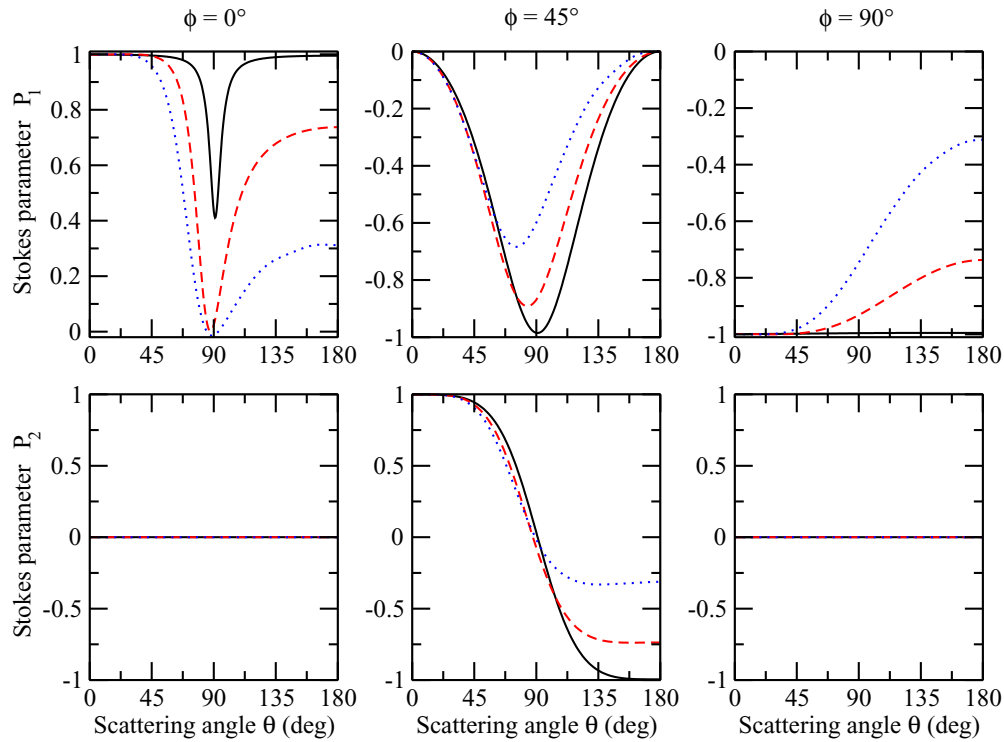


FIG. 4. (Color online) Stokes parameters P_1 (top row) and P_2 (bottom row) of elastically scattered x rays on hydrogenlike Xe^{53+} ions in their ground state. Calculations were performed for the same energies as above, $\hbar\omega = 1.1 I_{\text{th}}$ (solid line), $5 I_{\text{th}}$ (dashed line), and $10 I_{\text{th}}$ (dotted line), and for the emission angles $\phi = 0^\circ$ (left column), 45° (middle column), and 90° (right column) with regard to the reaction plane.

V. SUMMARY AND OUTLOOK

In summary, second-order perturbation theory and Dirac's relativistic equation have been employed to reinvestigate the

Rayleigh scattering of photons by hydrogenlike ions. In this analysis, attention was given to the angular distribution and linear polarization of the scattered light. We have shown, in particular, how all the (angular and polarization) properties

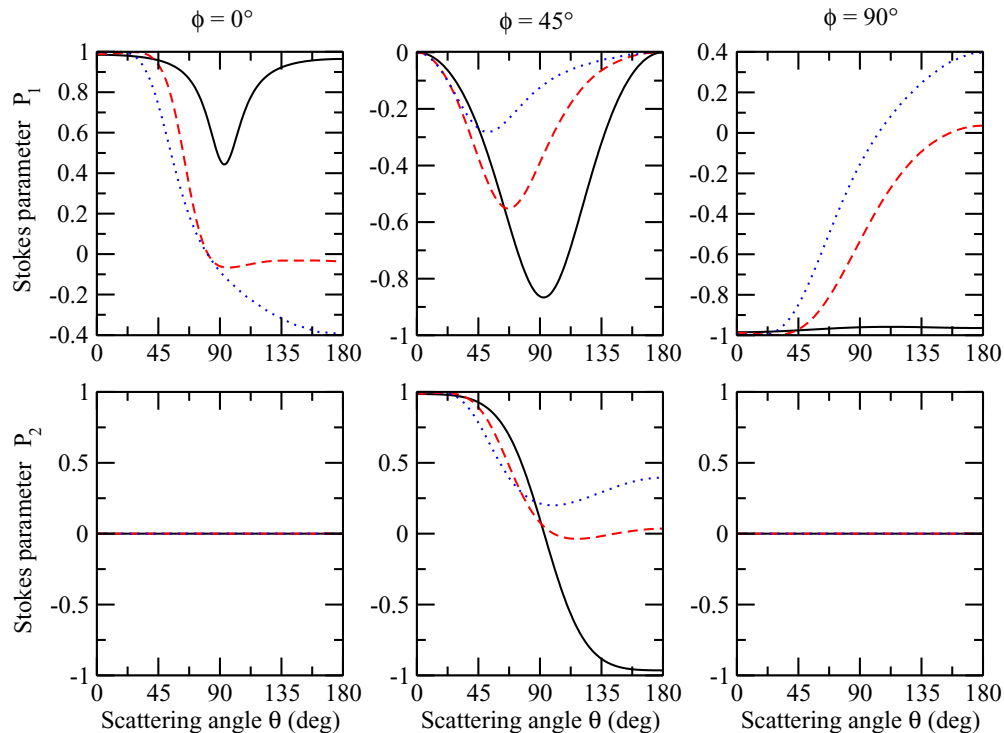


FIG. 5. (Color online) The same as Fig. 4, but for the Rayleigh scattering by hydrogenlike U^{91+} ions.

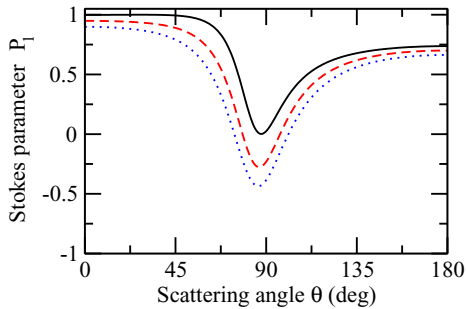


FIG. 6. (Color online) Stokes parameter P_1 of elastically scattered x rays within the (xz) reaction plane for hydrogenlike Xe^{53+} . Calculations were performed for energy $\hbar\omega = 5 I_{\text{th}}$ of the incident light and for various degrees of its linear polarization: $\mathcal{P} = 1$ (solid line), 0.95 (dashed line), and 0.9 (dotted line).

of the emitted radiation can be traced back to the differential (scattering) cross section, which depends on the wave and polarization vectors of both the incident and outgoing photons. The general formula for such a cross section was obtained by including also all higher-order (nondipole) effects in the electron-photon interaction.

Indeed, the derived expressions for the differential cross section and polarization parameters can be utilized to predict the properties of the Rayleigh scattered photons for an arbitrary polarization of the incident light and state of the target ion. In the present work, however, we have restricted our computations to the elastic K -shell scattering of *linearly* polarized light, a scenario which can be realized by combining modern ion-trap facilities with high-energy synchrotron radiation from sources such as PETRA III in Hamburg. Detailed calculations of the angular distribution and polarization (Stokes) parameters of outgoing x rays were performed for hydrogenlike neon, xenon, and uranium ions and for different photon energies. From the comparison of our fully relativistic calculations with the nonrelativistic dipole predictions, we explain and show explicitly how the properties of the scattered light are affected by the relativistic and nondipole effects. In particular,

we demonstrate here that, in addition to a strongly enhanced forward emission, these relativistic effects may result in a significant depolarization of the outgoing radiation. The depolarization is largest for the backward scattering but may also reach about 20% in the forward direction at emission angles $\theta \lesssim 45^\circ$. As expected, the deviation of our fully relativistic results from nonrelativistic data becomes most pronounced if the nuclear charge of the ions as well as the photon energy is increased. Besides the analysis of the relativistic and nondipole effects, we have demonstrated also that the linear polarization of the scattered photons may vary significantly if the incident light is incompletely polarized. Therefore, our calculations also clearly reveal the importance of a good polarization control of the light beams that are to be employed in future Rayleigh scattering experiments.

Although our present computations were carried out for hydrogenlike ions only, the theoretical background and expressions derived here can also be employed directly to explore the elastic photon scattering by neutral atoms. While for sufficiently hard x rays the major contribution to the scattering cross sections is expected to arise from the K -shell electrons, the study of interelectronic-interaction and outer-shell effects on the Rayleigh scattering would require computation of second-order amplitudes for complex (many-electron) atoms. These matrix elements can be evaluated in an accurate and efficient way by making use, for instance, of B splines and the multiconfiguration Dirac-Fock method. The first implementations for such relativistic many-body calculations of the angular and polarization properties of scattered photons are currently underway and will be presented in a forthcoming publication.

ACKNOWLEDGMENTS

This work has been supported by the Helmholtz Gemeinschaft (Nachwuchsgruppe VH-NG-421) and by the BMBF under Contract No. 05K13VHA. P.A. acknowledges the support of the German Research Foundation (DFG) within the Emmy Noether program under Contract No. TA 740 1-1.

-
- [1] W. Franz, *Z. Phys.* **98**, 314 (1935).
 - [2] P. P. Kane, L. Kissel, R. H. Pratt, and S. C. Roy, *Phys. Rep.* **140**, 75 (1986).
 - [3] S. C. Roy, R. H. Pratt, and L. Kissel, *Radiat. Phys. Chem.* **41**, 725 (1993).
 - [4] M. Y. Sfeir, F. Wang, L. Huang, C.-C. Chuang, J. Hone, S. P. O'Brien, T. F. Heinz, and L. E. Brus, *Science* **306**, 1540 (2004).
 - [5] A. I. Milstein and M. Schumacher, *Phys. Rep.* **243**, 183 (1994).
 - [6] S. C. Roy, L. Kissel, and R. H. Pratt, *Radiat. Phys. Chem.* **56**, 3 (1999).
 - [7] W. M. J. Veigele, *Atomic Data Tables* **5**, 51 (1973).
 - [8] L. Kissel, R. H. Pratt, and S. C. Roy, *Phys. Rev. A* **22**, 1970 (1980).
 - [9] W. Chitwattanagorn, R. B. Taylor, P. Teansomprasong, and I. B. Whittingham, *J. Phys. G* **6**, 1147 (1980).
 - [10] R. H. Pratt, *Radiat. Phys. Chem.* **74**, 411 (2005).
 - [11] N. Singha and S. Puri, *Radiat. Phys. Chem.* **75**, 2221 (2006).
 - [12] A. Costescu, K. Karim, M. Moldovan, S. Spanulescu, and C. Stoica, *J. Phys. B* **44**, 045204 (2011).
 - [13] L. Safari, P. Amaro, S. Fritzsche, J. P. Santos, and F. Fratini, *Phys. Rev. A* **85**, 043406 (2012).
 - [14] D. Brini, E. Fuschini, D. S. R. Murty, and P. Veronesi, *Nuovo Cimento* **11**, 533 (1959).
 - [15] D. R. S. Somayajulu and V. Lakshminarayana, *J. Phys. A* **1**, 228 (1968).
 - [16] S. C. Roy, B. Sarkar, L. D. Kissel, and R. H. Pratt, *Phys. Rev. A* **34**, 1178 (1986).
 - [17] F. Smend, D. Schaupp, H. Czerwinski, M. Schumacher, A. H. Millhouse, and L. Kissel, *Phys. Rev. A* **36**, 5189 (1987).
 - [18] Th. Stöhlker *et al.* (unpublished).
 - [19] U. Spillmann, H. Bräuning, S. Hess, H. Beyer, Th. Stöhlker, J.-Cl. Dousse, D. Protic, and T. Krings, *Rev. Sci. Instrum.* **79**, 083101 (2008).

- [20] G. Weber, H. Bräuning, S. Hess, R. Märtin, U. Spillmann, and Th. Stöhlker, *J. Instrum.* **5**, C07010 (2010).
- [21] N. L. Manakov, A. V. Meremianin, A. Maquet, and J. P. J. Carney, *J. Phys. B* **33**, 4425 (2000).
- [22] L. Safari, P. Amaro, S. Fritzsche, J. P. Santos, S. Tashenov, and F. Fratini, *Phys. Rev. A* **86**, 043405 (2012).
- [23] M. Gavrila, *Phys. Rev.* **163**, 147 (1967).
- [24] A. I. Akhiezer and V. B. Berestetskii, *Quantum Electrodynamics* (Wiley, New York, 1965).
- [25] N. L. Manakov, A. V. Meremianin, and A. F. Starace, *J. Phys. B* **35**, 77 (2002).
- [26] S. P. Goldman and G. W. F. Drake, *Phys. Rev. A* **24**, 183 (1981).
- [27] D. A. Varshalovich, A. N. Moskalev, and V. K. Khersonskii, *Quantum Theory of Angular Momentum* (World Scientific, Singapore, 1988).
- [28] P. Koval, S. Fritzsche, and A. Surzhykov, *J. Phys. B* **37**, 375 (2004).
- [29] A. Surzhykov, P. Indelicato, J. P. Santos, P. Amaro, and S. Fritzsche, *Phys. Rev. A* **84**, 022511 (2011).
- [30] W. H. McMaster, *Rev. Mod. Phys.* **33**, 8 (1961).
- [31] V. V. Balashov, A. N. Grum-Grzhimailo, and N. M. Kabachnik, *Polarization and Correlation Phenomena in Atomic Collisions* (Springer, Boston, 2000).
- [32] W. R. Johnson, S. A. Blundell, and J. Sapirstein, *Phys. Rev. A* **37**, 307 (1988).
- [33] C. Froese Fischer and F. A. Parpia, *Phys. Lett. A* **179**, 198 (1993).
- [34] P. Amaro, J. P. Santos, F. Parente, A. Surzhykov, and P. Indelicato, *Phys. Rev. A* **79**, 062504 (2009).
- [35] P. Amaro, A. Surzhykov, F. Parente, P. Indelicato, and J. P. Santos, *J. Phys. A* **44**, 245302 (2011).
- [36] P. J. Mohr, *Ann. Phys. (NY)* **88**, 52 (1974).
- [37] R. A. Swainson and G. W. F. Drake, *J. Phys. A* **24**, 95 (1991).
- [38] P. Koval and S. Fritzsche, *Comput. Phys. Commun.* **152**, 191 (2003).
- [39] V. A. Yerokhin and A. Surzhykov, *Phys. Rev. A* **81**, 062703 (2010).
- [40] Th. Stöhlker *et al.*, *Phys. Scr. T* **110**, 384 (2004).
- [41] S. Tashenov *et al.*, *Phys. Rev. Lett.* **97**, 223202 (2006).
- [42] J. Eichler and Th. Stöhlker, *Phys. Rep.* **439**, 1 (2007).